Biosensors and Bioelectronics 57 (2014) 96–102

Contents lists available at ScienceDirect

Biosensors and Bioelectronics

journal homepage: www.elsevier.com/locate/bios

Comparing label free electrochemical impedimetric and capacitive biosensing architectures

Flávio C.B. Fernandes, Adriano Santos, Denise C. Martins, Márcio S. Góes, Paulo R. Bueno *

Institute of Chemistry, University Estadual Paulista (UNESP, São Paulo State University), CP 355, CEP 14800-900 Araraquara, São Paulo, Brazil

ARTICLE INFO

Article history:
Received 7 December 2013
Received in revised form
22 January 2014
Accepted 24 January 2014
Available online 31 January 2014

Keywords:
Capacitance spectroscopy
Electrochemistry impedance spectroscopy
Biosensor
Immunosensor
Surface engineering

ABSTRACT

The transducer faradaic signals of molecularly receptive interfaces associated with specific target binding can be sensitively monitored by electrochemical impedance and/or capacitance spectroscopies. A comparative evaluation of both impedimetric (associated with charge transfer resistance) and capacitive (associated with faradaic density of states) approaches was undertaken using C-reactive protein (CRP) antigen and antibody interaction as biomolecular binding model. Aiming at constructing redox free (impedimetric) and redox tethered receptive (capacitive) interfaces engineered by self-assembly monolayer, CRP sensitivity and limit of detections were comparatively assessed regarding biosensor capabilities. Binding affinity constant between CRP and anti-CRP interfacial receptor sites were additionally evaluated by the Langmuir adsorption model. Both the impedimetric and capacitive approaches reported similar values of experimental analytical parameters albeit the latter was found to have the advantage of requiring no solution redox reporter thus making it highly suitable for use in multiplexing affinity arrays.

1. Introduction

In preparing sensorial interface for biological applications, the functionalization of electrode is seen to be primordial since metal interface by itself is generally regarded as a source of proteins denaturation besides the difficulty encountered with regard to the electronic binding between metal and protein (or biological entities) (Eddowes and Hill, 1977). N-alkanes with a thiol group at one end and a methyl, carboxyl or hydroxyl functionality at the other end have been frequently used to create a hydrophobic, negatively charged or hydrophilic surface, respectively (Poirier and Pylant, 1996). The carboxyl charge can be reversed by supplying electrolyte containing doubly charged metal ions such as Mg (Lu et al., 1996). Regarding immunosensor surface design specifically, the biological receptor attachment features such as orientation for the target to bind is key in determining the biosensor sensitivity and stability (Lu et al., 1996). Although many approaches for design or surface engineering have been discussed (Sassolas et al., 2012; Trilling et al., 2013), the self-assembled monolayers (SAMs) approach built by chemisorption between a gold surface and head group of a thiol molecule (Love et al., 2005; Ulman, 1996; Wink et al., 1997) has become one of the simplest and mostly adopted methodology currently employed in constructing receptive surface comprising the designing of electrochemistry, piezoelectric and optical transducing surface for biosensors applications (Chaki and Vijayamohanan, 2002).

Through the SAM surface functionalization approach, a well-defined, stable and oriented molecular film can be obtained with great versatility mainly in terms of usefulness and functionality (Chaki and Vijayamohanan, 2002; Love et al., 2005). For instance, it is worth mentioning the activation of a SAM with chelating groups such as 1-acetate-4-benzyl-triazacyclononane. In the presence of Ni, it is found to form a stable bond with a His-tag thereby assisting in the immobilization of His-tagged proteins on SAMs (Johnson and Martin, 2005). SAMs on Au have also been constructed from linear molecules derived from adamantane, conjugated aryl thiols and oligophenylene–vinylene (Armstrong et al., 2004).

The characteristics of alkanethiol SAMs have been investigated extensively (Love et al., 2005) using XPS (Dias et al., 2013), infrared (Porter et al., 1987) and Raman spectroscopy (Bryant and Pemberton, 1991) where the thiolate nature of the bound sulfur species has even been specifically confirmed by means of STM (Poirier and Pylant, 1996) and near-edge extended X-ray absorption fine structure (Hähner et al., 1992). Complementarily, we have recently introduced Capacitance Spectroscopy (CS) in another work where dipolar/electrostatic features of non-electroactive SAMs (named as SAMCS) are made to undergo characterization (Bueno et al., 2012; Bueno et al., 2013b). The theoretical framework of this technique, exemplified across a range of alkanethiol films (Goes et al., 2012), is fully aligned with yet more detailed than the classic Helmholtz plate capacitor model of such interfaces and is found to provide clearer resolution of the trends of distortion effects in both capacitance and resistance in electroactive monolayers (Boubour and Lennox, 2000; Eckermann et al., 2010).

In exemplifying SAMs usefulness for biosensor applications, Quartz Crystal Microbalance (QCM) based bio interfaces have been constructed by the immersion of the quartz crystal chip (with Au

* Corresponding author. Tel.: +55 16 3301 9642; fax: +55 16 3322 2308.
E-mail address: prbueno@iq.unesp.br (P.R. Bueno).

0956-5663/$ - see front matter © 2014 Elsevier B.V. All rights reserved.
http://dx.doi.org/10.1016/j.bios.2014.01.044

electrode interfaces) in carboxilated terminal thiol solution where the receptor molecule is attached directly over the Au surface of the QCM and binding event to this receptive interfaces is detectable by measuring the mass increase as a consequence of oscillatory frequency change (Cooper and Singleton, 2007). Equivalently SPR (Surface Plasmon Resonance) devices have been constructed (Reddy et al., 2012), though with comparable lower sensitivity (Lum et al., 2012). Both QCM and SPR approaches although sensible and label free are not readily applied in any high throughput or practical *point of care* settings. Electrochemical approaches such as amperometric, voltammetric as well as electrochemical impedance spectroscopy (EIS) are alternatively used among which the EIS is known to offer the most suitable tool when seeking for methodologies with high levels of sensitivity for the detection of biomarkers without target labeling, pre-synthesis, or the use of sandwich formats requiring two specific antibodies per target. (Daniels and Pourmand, 2007; Johnson et al., 2012; Lisdat and Schaefer, 2008).

The use of EIS transducer signal in biological sensorial applications is based on the interaction between the biological receptor and the target species (antigen–antibody, for example) recruited from the solution by causing a change on interfacial electron transfer kinetics between a redox probe in solution and metallic electrode sites. This electrochemical change is then detectable by monitoring the charge transfer resistance R_{ct} that increases in the same proportion given the increase in the quantity of targets bound to the receptive surface (Elshafey et al., 2013; Hu et al., 2013; Lisdat and Schaefer, 2008; Ohno et al., 2013). Usually the variation of ΔR_{ct} is percentually measured with respect to a reference resistance value. The percentage of response is calculated as $R_n\,\% = 100\%\,(R_n - R_0)/R_0$ where R_0 is the specific interfacial response for zeroed target concentration (R_0), i.e., the blank response reference. Also one may use QUOTE, i.e. the relative no percentage response.

Using the impedimetric based spectroscopy as transducing signal, a novel and label free means of detecting specific protein targets at suitably modified electrodes has been reported recently (Fernandes et al., 2013) with good reproducibility and sensitivity utilizing a fully capacitive based response of a redox modified electrode where the sensitivity of this redox-receptive interface to changes on the density of states (DOS) occupancy is known to be the key operational aspect of this bio sensorial interface as will be detailed herein. In contrast to the traditional previously mentioned impedimetric method, no redox probe (or redox electrochemical pair) is added to the screened solution thus making this methodology (Electrochemical Capacitance Spectroscopy, ECS) experimentally simple, with optimized frequency, and likely to be equally applicable to a broad range of target/receptor combinations in a very potential and suitable platform for multiplexing applications (see Fig. 1 for details on differences between EIS and ECS approaches from surface chemistry point of view).

Based on what was stated above, the main purpose of the present work is to compare the operational principle of the impedimetric and capacitive based biosensing interfaces regarding the surface chemistry designing. Furthermore, it will also be comparatively demonstrated that capacitive transducing signal is suitable for the determination of affinity constant between the target and receptor with the aid of the Langmuir isotherm. The applicability of the said technique stands to be very important when it comes to designing future protein affinity microarrays.

2. Experimental procedures

2.1. Electrode surface preparation

The preparation of the gold surface was made by mechanical polishing with aluminum oxide pads (1 μm, 0.3 μm and 0.05 μm)

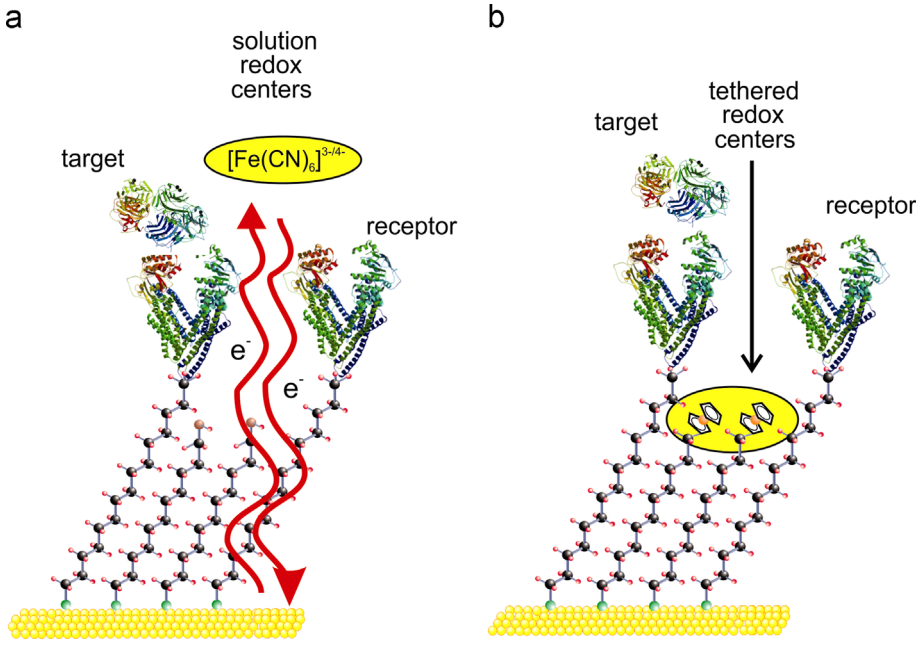

Fig. 1. Schematic representation of two different approaches to study biomolecular target and receptor interaction for sensor or binding interaction study. In (a) it is schematically shown surface constructed into gold surface by mixed thiol SAM structures where 1-pentadecanethiol serves as receptor supportive layer and 11-mercapto-1-undecanol non electroactive layer spacer. In this SAM structure faradaic impedimetric measurements can be carried out by using a probe redox in solution, exemplified here as $[Fe(CN)_6]^{3-/4-}$. The non electroactive monolayer in (a) intermediates electron transfer (as show by the red arrows) between the redox couple in solution and Au states and this is related to electron transfer kinetics throughout R_{ct}. The latter increases when the target concentration is increased. In (b) it is schematically shown surface constructed into gold surface by mixed thiol SAM structures where 1-pentadecanethiol serves as receptor supportive layer and and 11-ferrocenyl-undecanethiol serve as electroactive layer spacer and capacitive redox centers given rise to redox capacitance, C_r.

with decreasing particles sizes. Sonication in water to remove adhered particles was performed between polishing steps. The electrodes surfaces were then electrochemically polished in deaerated NaOH 0.5 M (−1.5 V and −0.5 V at a scan rate of 50 mV s^{-1}) and subsequently in deaerated 0.5 M H_2SO_4 (−0.2 V and 1.5 V at a scan rate of 100 mV s^{-1}) until the stabilization of the gold reduction peak in CV is attained (around 50 cycles). Following the electrochemical polishing steps, electroactive areas were evaluated by mathematical integration of the cathodic peak with potential from gold electropolishing voltammograms and converted to the real surface area using a conversion factor of 410 μC cm^{-2} (Trasatti and Petrii, 1991). As the roughness factor needed to be controlled, it was kept within the range of 1.1–1.4 in all the measurements carried out. Finally, the polished gold electrode was characterized by Cyclic Voltammetry (CV), Electrochemistry Impedance Spectroscopy (EIS) and Electrochemical Capacitance Spectroscopy (ECS).

2.2. Surface engineering for impedimetric and capacitive biosensoring and binding affinity

EIS and ECS have different concepts as will be stated herein. Each approach needs specific surface architecture according to either resistive or capacitive transducer signal. Regardless of the operation mechanism, we have constructed protein receptive binding interfaces whose target was C-reactive protein (CRP), elected as our biological model. CRP is an important biomarker for cardiac events and inflammation (Bryan et al., 2013; Dotsenko et al., 2007), where its early quantification can generally be considered indispensable. Currently, the methods based on turbidimetric (Roberts et al., 2000) and nephelometric (Roberts et al., 2001) techniques for clinical CRP detection have been employed or human CRP enzyme-linked immunosorbent assay (ELISA) kits. The said methods are robust for the screening of CRP, however, these approaches suffer from limitations of sensitivity, cost, selectivity and processing time (Pearson et al., 2004). Thus, cheaper, quicker and more sensitive alternative label free methods are required for the determination of the CRP making the latter a good biological model for the proof of concepts. Three different surface chemistry architectures (SCA) named SCA-1, SCA-2 and SCA-3 were strategically assembled to be comparatively studied using the EIS and the ECS. SCA-1 was constructed for the EIS while SCA-2 and SCA-3 for the ECS analysis (see Fig. 1 for more illustrative information). SCA-1 is compared with SCA-2 and SCA-3. The SCA-2 and SCA-3 were found to differ only by the way the biological receptor was attached to the SAM as elucidated as follows.

A freshly cleaned (mechanically and electrochemically polished) Au electrode (treated as previously described) was immersed for 16 h in a solution containing the appropriate thiols in ethanol P.A. for each type of the SCA. SCA-1 was assembled by immersing Au electrode in a mixed solution of 0.2 mM 1-pentadecanethiol (*for hydrophobic* CRP antibody attachment) and 2.0 mM 11-mercapto-1-undecanol (used as non electroactive spacer). For the SCA-2, Au electrode was immersed in a mixed solution of 0.2 mM 1-pentadecanethiol (*for hydrophobic* CRP antibody attachment) and 2.0 mM 11-ferrocenyl–undecanethiol (now used as electroactive spacer) and electrolyte. Finally, SCA-3 was similarly assembled in the similar pattern as SCA-2, i.e., by immersing Au electrode in a mixed solution of 0.2 mM 16-mercaptohexadecanoic acid (*for covalent* CRP antibody attachment) and 2.0 mM 11-ferrocenyl–undecanethiol. It is worth noting that for the SCA-2 and SCA-3, ferrocene group was utilized as a confined probe redox as required for the ECS analysis (Fernandes et al., 2013). The SCA-2 and SCA-3 were found to be equivalent, differing with regard to the attachment of biological receptor to the SAM interfaces with the former being hydrophobic and the latter being covalent. In all cases, after the SAM formation, the electrodes were washed using alcohol, Milli-Q water (18.2 MΩ at 25 °C; Millipor, Simplicity System, Bedford, MA, USA) and dried under nitrogen gas.

In the SCA-1 and SCA-2, the receptive surfaces were prepared by the direct immersion of the electrodes in 200 μL of a 1 μM of anti-CRP in phosphate buffered saline (PBS), pH 7.4, for 1 h prior to electrochemical analysis. For the SCA-3, a proper activation of the SAM through the standard EDC/NHS bioconjugation chemistry method was done using a solution of 0.4 M EDC and 0.1 M NHS for 30 min prior to the covalent attachment of the antibody. Afterwards, aiming at blocking unspecific sites, this anti-CRP functionalized electrode was immersed in 200 μL of BSA 0.1% solution in PBS, pH 7.4, for 1 h at 25 °C.

Before electrochemical characterization, for all methodologies used, CRP aliquots (20 μl) were added to interact (incubation) with the anti-CRP receptive interface in the concentrations ranging from 0.5 nM to 10.0 nM in PBS (pH 7.4). For each concentration the electrode was then rinsed with PBS and EIS, ECS and CV measurements were taken.

2.3. Construction of receptive interfaces and standard curve

Electrochemical characterization in SCA-1 was conducted using EIS and CV measurements recorded in KNO_3 1 mol L^{-1} supporting electrolyte containing 1 mM $[Fe(CN)_6]^{3-/4-}$ as redox probe. For the SCA-2 and SCA-3, the electrochemical measurements (primarily ECS) were recorded in a supporting electrolyte of 20 mM $TBAClO_4$ (tetrabutylammonium perchlorate) dissolved in acetonitrile and H_2O (20:80) without any probe redox in solution. For all the methods, CV was performed at a scan rate of 100 mV s^{-1} between 0.0 V and 0.7 V relative to Ag/AgCl.

In order to verify the specific interaction, control surface analysis was performed. For this purpose, standard plots were constructed adding concentrations of the target above the sensor without immobilizing the antibody (the blank signal). The target detection limits were calculated based on the definitions as three times the standard deviation of the blank, whereas the quantification limits were obtained being ten times the standard deviation of the blank, in line with the determination of the IUPAC (Long and Winefordner, 1983).

2.4. Electrochemical measurements

An AUTOLAB potentiostat model PGSTAT30 with FRA module controlled by NOVA program was used for all electrochemical measurements. A three electrode setup was used for all measurements, consisting of a 2.0 mm diameter gold working electrode from METROHM, a platinum mesh counter electrode and an Ag|AgCl 3 mol L^{-1} KCl reference electrode. EIS measurements were conducted in a frequency range of 10 mHz–1 MHz with a RMS amplitude of 3 mV (or 10 mV peak to peak). All measurements were performed in triplicate. The ECS analysis was done obtaining $C^*(\omega)$ by means of impedance $Z^*(\omega)$ using the following relationship $C^*(\omega) = 1/i\omega Z^*(\omega)$, in which ω is the angular frequency and $i = \sqrt{-1}$ (Bueno et al., 2012).

All reagents described in this section (this work) were purchased from Sigma-Aldrich.

3. Results and discussion

3.1. Theoretical concepts and backgrounds

With regard to the use of EIS to follow biological binding events, the application of redox probe to analytical solution prior

to analysis is required (Elshafey et al., 2013; Hu et al., 2013; Lisdat and Schaefer, 2008; Ohno et al., 2013) and the sensorial electro analytical signal is based on ΔR_{ct} changes, i.e., it depends on the electron transfer impediment ability of biological interface as a function of the binding event. On the other hand, with regard to the ECS, the sensorial electro analytical signal is capacitive based (charge storage) and not resistive based (redox impediment). The capacitive signal is also faradaic (or redox) based and was denoted in previous works as faradaic (or redox) capacitance, C_r (Bueno et al., 2012). The signal is essentially based on ΔC_r changes (Fernandes et al., 2013). Redox capacitance is not a common electrostatic capacitance whose potential depends only on dimensions but instead it depends largely on the electrochemical potential. In short, C_r is related to the redox density of states, DOS, whose occupancy, considering one energy state level, is given by

$$C_r = \frac{e^2 \Gamma}{k_B T} f(1-f) \quad (1)$$

where $f = n/ = F(E_r, \mu_e) = \{1+\exp[(E_r-\mu_e)/k_B T]\}^{-1}$ is the occupation function given by the Fermi Dirac function, e is the elementary charge, k_B the Boltzmann constant, T the absolute temperature and Γ is the redox molecular surface coverage. Note in Eq. (1) that C_r is maximized when $f = 1/2$ and $f(1-f) = 1/4$, i.e., at the half-wave potential. In addition, it can be noted that f is a function of the electron chemical potential, μ_e, and E_r, i.e., the potential of redox centers that controls the occupation according to the redox potential level by $\Delta G = E_r - \mu_e$.

As described in the experimental section, both the EIS and ECS are sustained on the same mathematical principles, i.e., on the measurement of interfacial electrical transfer function known as $Z^*(\omega)$. However, in analyzing the corresponding transfer function by the ECS point of view, the signal is mathematically converted to $C^*(\omega)$ (see Section 2) where C_r can be readily obtained by Nyquist or Bode diagram analysis. Although mathematically equivalent, the ECS representation unveiled C_r physical term.

Essentially, from a physical chemistry point of view, for C_r to be a detectable signal, the surface chemistry must be accordingly engineered in a way that confined electron transfer is possible (or redox charge stored in the interface, i.e., electrochemical energy storage is allowed). Therefore, the redox capacitance is associated with the quantum nature (Bueno and Davis, in press). of electrochemistry confinement at molecular scale and will only be present if the charge can be chemically (not only electrostatic) stored between electrode and molecular layer. When molecular redox levels are tethered to a metal electrode surface, as is the case of surface chemistry depicted in Fig. 1b, C_r can be detected as a consequence of the electrochemical energy storage capability of this interface. In the absence of tethered redox levels, as is the case of surface chemistry depicted in Fig. 1a, the electrochemical energy storage is impossible so that C_r is absent (see Fig. 2d and Fig. 3). In the latter depicted surface, any energy driven by faradaic current will be lost into R_{ct} component to solution redox levels (in a diffusive driven electron transfer regime) and cannot be energetically stored onto the surface (Bueno et al., 2013a).

In terms of electrochemical equivalent circuit analysis, the EIS characteristics of SCA-1 based interfaces are, at all points, well described by the equivalent circuit of Fig. 3 (enabling R_{ct} to be precisely obtained by fitting analysis). It is noteworthy that the dipolar relaxation characteristics of the supporting SAM layer adjusted within R_t and C_t, are considered within a Randle modified equivalent circuit (see Fig. 3a). Without an adequate consideration of these monolayer dielectric contributions, the error in the calculation of R_{ct} is seen to be markedly higher. These SAM fingerprint terms and meanings were previously well described (Bryan et al., 2013; Bueno et al. 2013b; Goes et al. 2012). It is also important to point out that R_{ct}, as monitored through low frequency, impedance sampling measures the redox probe diffusive access to the underlying gold surface besides the charge transfer (Bryan et al., 2013a; Bueno et al., 2013b; Goes et al., 2012). The capacitive features of this interface (SCA-1) do not respond in any sensitive or calibratable manner to the CRP binding as was demonstrated in a previous work (Fernandes et al., 2013). This can be equivalently confirmed from the experimental results shown in Fig. 2a and b where, respectively, in the Nyquist impedimetric diagrams, the changes in R_{ct} are evident for the SCA-1, whereas no change is observed in the Nyquist capacitive representation.

On the other hand, as evidenced in Fig. 2c and d, for redox tethered sites, the capacitive analysis is detectable within the change in C_r but no variation is observed in R_{ct} in the Nyquist impedimetric diagrams. The differences in terms of equivalent circuit element between the impedimetric and capacitive approaches are observable by the replacement of Warburg term by C_r (Fig. 3). In other words, as predictable, SAMs containing tethered redox centers are diffusionless electrochemical systems (Bueno et al., 2012; Laviron, 1979). The physical meaning of C_r is essential for a comprehensible electro analysis of electroactive SAM for any kind of applications (Bueno et al., 2012; Bueno et al., 2013b)

In summary, both R_{ct} and C_r can be used for sensorial properties depending on the surface chemistry architecture. On one hand, for R_{ct} based sensorial signal, the surface chemistry optimization is based on chemically dependent steric (i.e., impedimetric) access of redox probe to metallic states intermediated by the receptive surface and the target binding occupations. On the other hand, for C_r sensorial signal, the transducing process is controlled by the redox states occupation tethered to metallic electrode. The occupation of these redox states is controlled by redox DOS occupancy as a function of target binding to adlayer.

3.2. Surface chemistry and biosensoring

As discussed in the previous section, the changes in C_r, as measured in mixed receptive and redox active confined monolayer architecture as a function of target binding, reflects the sensorial capability of ECS for biosensor applications (Fernandes et al., 2013).

Using CRP (target) and anti-CRP (receptor) biomolecular model, we compared herein the EIS and ECS sensorial approaches, i.e., the limit of detection (LOD), limit of quantification (LOQ), repeatability and sensibility were contrasted. The comparative values for SCA-1, SCA-2 and SCA-3 are shown in Table 1. These values were obtained through the analytical curve shown in Fig. 4.

From Fig. 4, it can be noted that the angular coefficient (providing sensibility) was influenced by the surface chemistry. As pointed out in the experimental section, the anti-CRP receptor was hydrophobically attached to the SCA-1 and SCA-2 receptive interfaces for the direct comparison of the EIS and ECS approaches, while covalent attachment was used in SCA-3 in order to compare differences in SCA-2 and SCA-3 according to the binding kind used in anti-CRP attachment. The robustness of the SCA-3 approach is observed owing to the lower standard deviation among the triplicates (less than 7% comparatively to about an average value of 28% for the SCA-1 and SCA-2 interfaces). The higher robustness of SCA-3 was expected in line with literature observations (Sassolas et al., 2012). However, it is also known that surface chemistry methodologies based on hydrophobic attachment of receptor can lead to higher sensibilities (Sassolas et al., 2012) (as indeed confirmed in Table 1).

The higher stability and the minor sensibility obtained for the SCA-3 are associated with the anti-CRP chemical immobilization. The covalent immobilization (of the SCA-3 approach) leads to a

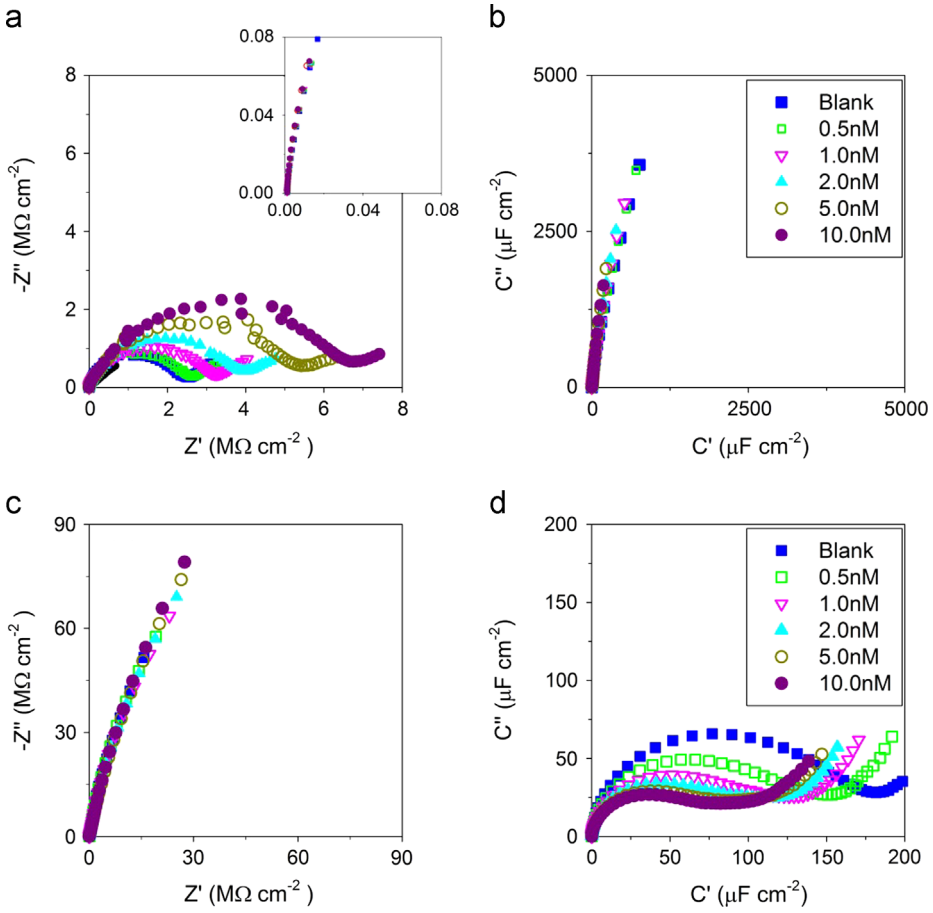

Fig. 2. Typical (a) impedimetric and (b) capacitive Nyquist diagrams obtained for SCA-1. Note here that (b) was constructed by converting impedance into capacitance as explained in the experimental section. The impedimetric analysis of (a) is promptly used to obtain ΔR_{ct} as a function of target concentration as indicated in the inset in (b). R_{ct} is obtained from the value of the diameter of the impedimetric Nyquist semicircle in (a). Note that there are no apparent changes on the Nyquist capacitive diagrams as expected according to what was explained in the main text (see Fig. 3 for more details about equivalent circuit). On the other hand, for the SCA-2 and SCA-3 receptive surfaces, typical (c) impedimetric and (d) capacitive Nyquist diagrams of the interfaces demonstrate there is no detectable change in impedance, meanwhile they are clear in the capacitance representation. Therefore, for the SCA-2 and SCA-3 redox confined or tethered receptive interfaces, the ECS instead of the EIS is seen to be clearly the most suitable approach. In using the ECS, $1/\Delta C_r$ can be promptly obtained as analytical signal (see Figs. 4 and 5 for more comparative details). C_r values are obtained from the diameter of the semicircle in Fig. 2d. All plots shown in this figure are mean values of measurements performed in three different receptive interfaces independently constructed.

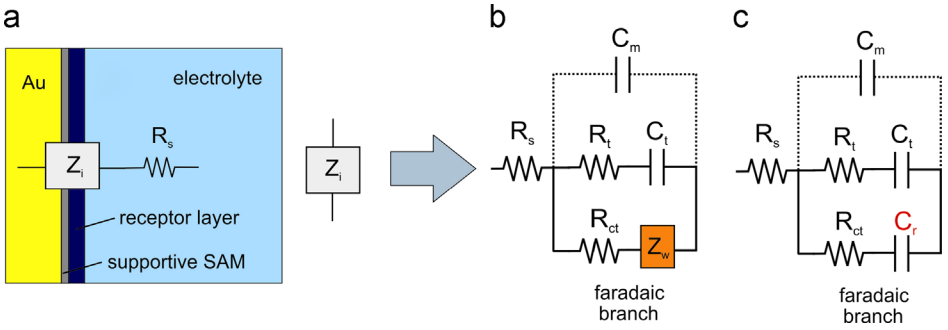

Fig. 3. (a) Schematic representation of the interfacial impedance of the CRP receptive interfaces used herein. (b) The equivalent circuit capable of modeling impedimetric biosensor data (SCA-1). The Warburg element (Z_w) accounts for the bulk diffusion characteristics of the redox probe and R_{ct} is the redox charge transfer resistance. The electrolyte resistance (R_s) is modeled in series with the above total interfacial impedance (see (a)) and generally it is not important in the prevaling analysis once it does not vary. (c) Is the appropriate equivalent circuit capable of modeling capacitive biosensor data (SCA-2 and SCA-3). Note that interfacial capacitance of a monolayer dielectric modified electrode is defined by two series capacitances, those of the monolayer (C_m) and of the double-layer (C_{dl}) where $C_{dl} \gg C_m$, meaning C_m dominates in analyses and is, therefore, the only capacitance represented in the equivalent circuit showed here. Furthermore, $C_m \ll C_t$ in a way that R_t and C_t control the monolayer dielectric (non faradaic) response (Goes et al., 2012; Lin et al., 2008; Lin et al., 2010; Romaner et al., 2008; Sondag-Huethorst and Fokkink, 1995).

decrease in unspecific interactions (confirmed by the small standard error obtained) but is found to provoke conformational changes of the receptive species (anti-CRP), decreasing the accessibility to the binding site which in turn leads to a reduction in the surface sensitivity.

The specificity between the CRP and its receptive surface was analyzed as can be observed in Fig. 4 for all the surfaces. As can be noted, no significant dependence and differences between the surface chemistries or receptor immobilization methods were observed, confirming the specificity between the CRP and anti-CRP receptive

surfaces. All the receptive surfaces showed promising LOD and LOQ values for CRP. LOQ shows a higher dependence (variability) on the surface chemistries compared to LOD.

In summary, immunosensors receptive interfaces can be designed either using the impedimetric approach (SCA-1) or the capacitive (SCA-2 and SCA-3) provided that the technique adopted presents suitable LOD and LOQ values. The capacitive based immunosensors are advantageous once this approach does not require the use of a solution redox probe.

3.3. Surface chemistry architectures and Langmuir isotherms

The usefulness of switching between EIS and ECS depends on the surface chemistry architecture (redox probe in solution or confined), that is to say, it depends on the interfacial measurements of resistance (redox probe in solution) or capacitance (redox confined). In both situations, it would be useful to state how these surface chemistry architectures are comparatively able to measure molecular or biological binding affinity constant between a solution target and receptor bound to the surface, i.e., the affinity constant (herein the affinity between anti-CRP and CRP, K_a).

Physically it is suitable to assume occupational functions for receptor sites. The most used model is the Langmuir adsorption isotherm. By using the Langmuir isotherm, it is understood that there are two possible independent and not correlated situations, i.e., unoccupied (R) and occupied (RT) receptor sites. Essentially, R represents the receptor site available to target binding. The dynamic equilibrium between R and RT for a target T to bind according to the Langmuir isotherm presumptions are then described by

$$R+T \rightleftharpoons RT \tag{2}$$

Table 1
Analytical parameters for the electrochemical determination of CRP protein in PBS buffer (pH 7.4).

	SCA-1	SCA-2	SCA-3
Linear range (nM)	0.5–10	0.5–10	0.5–10
C. Coefficient (R^2)	0.97	0.99	0.98
Sens. (L nmol^{-1} ΔR)	5540	2515	1248
L.O.D (nmol L^{-1})	0.265	0.200	0.240
L.O.Q (nmol L^{-1})	0.760	0.600	0.315
K_a (L mol^{-1})	$(7.6 \pm 0.2) \times 10^8$	$(5.4 \pm 0.5) \times 10^8$	$(5.0 \pm 0.3) \times 10^8$

The affinity constant, K_a, is then given by

$$K_a = \frac{[RT]}{[R][T]} \tag{3}$$

where [ ] stands for concentration. Assuming a surface coverage occupation percentage given by θ and a percentage of available sites as $1-\theta$, Eq. (3) can be rewritten as

$$K_a[T] = \frac{\theta}{1-\theta} \tag{4}$$

In solving Eq. (4) for θ we have

$$\theta = \frac{K_a[T]}{1+K_a[T]} \tag{5}$$

The biomolecular surface coverage, Γ (mol cm^{-2}), is proportional to θ. So, it can be assumed that $\Gamma = \theta\Gamma_m$, where Γ_m is the maximum amount of adsorption probability when θ approaches a unit, hence

$$\Gamma = \frac{\Gamma_m K_a[T]}{1+K_a[T]} \tag{6}$$

Eq. (6) can be linearized as

$$\frac{[T]}{\Gamma} = \frac{[T]}{\Gamma_m} + \frac{1}{K_a\Gamma_m} \tag{7}$$

K_a can be easily determined by the quotient between the angular $(1/\Gamma_m)$ and linear $(1/K_a\Gamma_m)$ coefficients.

Therefore, an increase in Γ implies a proportional increase in R_{ct} and a decrease in C_r. The increase in R_{ct} is due to an increase in the impediment of the interface for electron transfer upon the formation of RT (EIS, see Fig. 1a). On the other hand, as R is occupied by T forming RT according to Eq. (2), the number of occupied redox centers decreases (redox DOS decreases), which is experimentally detected by a decrease in C_r values. Consequently Eq. (6) can be rewritten as

$$\frac{[T]}{\Delta R} = \frac{[T]}{\Delta R_m} + \frac{1}{K_a \Delta R_m} \tag{8}$$

where ΔR was previously defined as the relative no percentage response that was accordingly used to construct the linear curves shown in Fig. 5. In this figure ΔR for EIS is ΔR_{ct} (Fig. 1a) and for ECS approach ΔR is $1/\Delta C_r$ (Fig. 1b) given that an increase in target binding causes a decrease in C_r.

The presumptions were validated and K_a was determined for EIS and ECS for the same binding molecular model. The K_a obtained values were $(7.6 \pm 0.2) \times 10^8$ L mol^{-1}, $(5.4 \pm 0.5) \times 10^8$ L mol^{-1} and $(5.0 \pm 0.3) \times 10^8$ L mol^{-1} respectively for SCA-1, SCA-2 and SCA-3. The similarity of the K_a values strongly provide

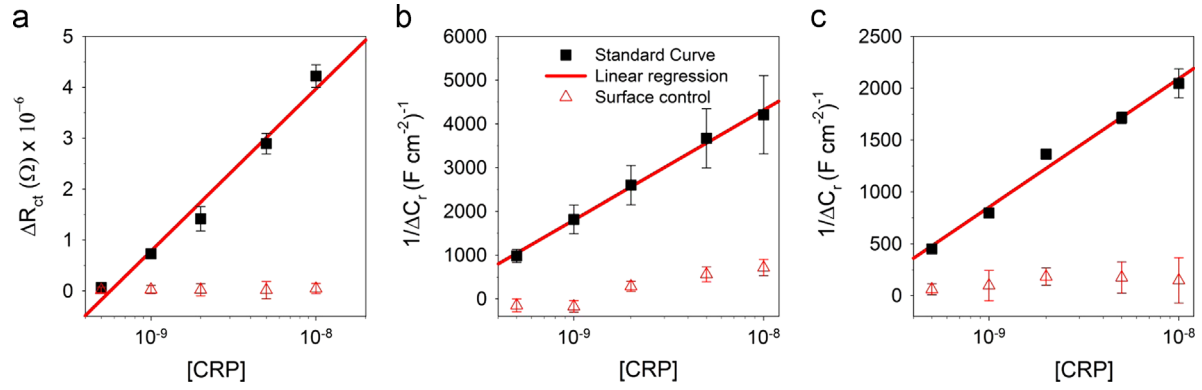

Fig. 4. (a) Analytical curve constructed based on ΔR_{ct} response of SCA-1 receptive interface plotted against logarithmic of CRP concentration. (b) Analytical curve constructed based on $1/\Delta C_r$ as a function of logarithmic of CRP target concentration for SCA-2 receptive surface. (c) Is the same as (b) but based on a receptive interface where receptors were attached covalently (SCA-3 surface) in contrast to hydrophobic attachment used in SCA-2. The linear regression adjustments for all different surfaces are higher than 0.97. The surface controls showed in each plot evidences all receptive surfaces respond specifically to CRP. The error bars indicate variance across triplicate measurements (i.e. three independently prepared assaying receptive surfaces).

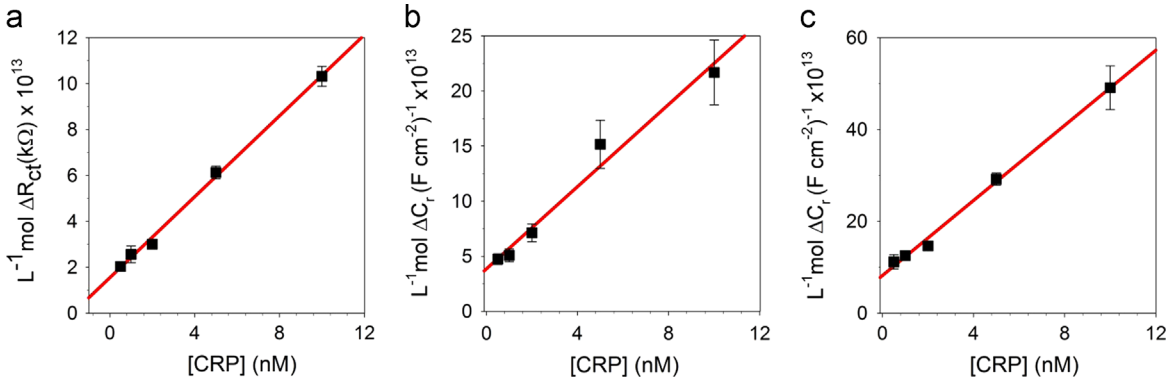

Fig. 5. Linear form of the Langmuir isotherm obtained for (a) impedimetric immunosensor with hydrophobic immobilization of the CRP, SCA-1; (b) capacitive immunosensor with hydrophobic immobilization of the CRP, SCA-2, and (c) capacitive immunosensor with covalent attachment of the CRP, SCA-3. The plots are appropriate for determining the affinity constant between the CRP and the anti-CRP receptive surface, K_a, according to Eq. (6). The linear regression adjustments for all different surfaces are higher than 0.97. By the K_a values obtained and displayed in Table 1 it is possible to infer that they are all equivalent within experimental error, as should be according to the premises of Langmuir model, meaning K_a is a constant that depends on binding itself and here it is independent of interface differences or transducing signal. The error bars indicate variance across triplicate measurements (i.e., three independently prepared assaying receptive surfaces).

evidence for the fact that biological affinity is independent of chemistry or transducer principle, i.e., independent of EIS or ECS approaches.

4. Conclusions

The present work sought to evaluate three different surface chemistries aiming at quantifying a biological target electro-analytically in a physiological environment. CRP protein was used as target to compare EIS and ECS electro-analytical approaches. LOD and LOQ of three engineered surfaces were found to present suitable values for immunosensors applications regardless of the approach adopted be it EIS or ECS. Furthermore, biochemistry affinity, K_a, was shown to be independent of engineered surface or transducer signal (resistive or capacitive).

The redox capacitive biosensor approach is based on tethered redox centers within the SAM and its electrochemical occupancy is affected by the change in its environment with the binding of the target. In contrast, impedimetric based biosensors depend on how the communication between the redox probe in solution and the metallic centers is impeded by the target binding. Both approaches are known to be versatile tools in the development of biosensors with good limits of detection and quantification. However, capacitive based sensors bear greater merit owing to the fact that they do not need a redox probe in solution, which helps to minimize the sample manipulation and thus making them ideal for point of care analyses.

Acknowledgements

This work was supported by the São Paulo state research funding agency (FAPESP) and São Paulo State University (UNESP) grants. Flávio Bedatty Fernandes acknowledges the CAPES (Coordination for the Improvement of Higher Level – or Education – Personnel) for his Ph.D. scholarship and grants.

References

Armstrong, F.A., Barlow, N.L., Burn, P.L., Hoke, K.R., Jeuken, L.J.C., Shenton, C., Webster, G.R., 2004. Chem. Commun. 3, 316–317.
Boubour, E., Lennox, R.B., 2000. Langmuir 16 (9), 4222–4228.
Bryan, T., Luo, X., Bueno, P.R., Davis, J.J., 2013. Biosens. Bioelectron. 39 (1), 94–98.
Bryant, M.A., Pemberton, J.E., 1991. J. Am. Chem. Soc. 113 (22), 8284–8293.
Bueno, P.R., Davis, J.J. Anal. Chem., in press, http://dx.doi.org/10.1021/ac4031708.
Bueno, P.R., Benites, T.A., Góes, M.S., Davis, J.J., 2013a. Anal. Chem.
Bueno, P.R., Davis, J.J., Mizzon, G., 2012. J. Phys. Chem. C 116 (30), 8822–8829.
Bueno, P.R., Fabregat-Santiago, F., Davis, J.J., 2013b. Anal. Chem. 85 (1), 411–417.
Chaki, N.K., Vijayamohanan, K., 2002. Biosens. Bioelectron. 17, 1–12.
Cooper, M.A., Singleton, V.T., 2007. J. Mol. Recogn. 20, 154–184.
Daniels, J.S., Pourmand, N., 2007. Electroanalysis 19 (12), 1239–1257.
Dias, D., Hasse, U., Fricke, K., do Nascimento, P.C., Scholz, F., 2013. J. Electroanal. Chem. 690, 121–126.
Dotsenko, O., Chackathayil, J., Lip, G., 2007. Expert Rev. Mol. Diagn. 7 (6), 693–697.
Eckermann, A.L., Feld, D.J., Shaw, J.A., Meade, T.J., 2010. Coord. Chem. Rev. 254 (15–16), 1769–1802.
Eddowes, M.J., Hill, H.A.O., 1977. J. Chem. Soc. Chem. Commun. 21, 771b–772b.
Elshafey, R., Tlili, C., Abulrob, A., Tavares, A.C., Zourob, M., 2013. Biosens. Bioelectron. 39, 220–225.
Fernandes, F.C.B., Góes, M.S., Davis, J.J., Bueno, P.R., 2013. Biosens. Bioelectron. 50 (0), 437–440.
Goes, M.S., Rahman, H., Ryall, J., Davis, J.J., Bueno, P.R., 2012. Langmuir 28 (25), 9689–9699.
Hu, Y.F., Zuo, P., Ye, B.C., 2013. Biosens. Bioelectron. 43, 79–83.
Hähner, G., Kinzler, M., Thümmler, C., Wöll, C., Grunze, M., 1992. JVST A 10 (4), 2758–2763.
Johnson, A., Song, Q., Ferrigno, P.K., Bueno, P.R., Davis, J.J., 2012. Anal. Chem. 84 (15), 6553–6560.
Johnson, D.L., Martin, L.L., 2005. J. Am. Chem. Soc. 127 (7), 2018–2019.
Laviron, E., 1979. J. Electroanal. Chem. 101 (1), 19–28.
Lin, J., Merzlyakov, M., Hristova, K., Searson, P., 2008. Biointerphases 3 (2), FA33–FA40.
Lin, J., Szymanski, J., Searson, P.C., Hristova, K., 2010. Langmuir 26 (14), 12054–12059.
Lisdat, F., Schaefer, D., 2008. Anal. Bioanal. Chem. 391 (5), 1555–1567.
Long, G.L., Winefordner, J.D., 1983. Anal. Chem. 55 (7), 712–724.
Love, J.C., Estroff, L.A., Kriebel, J.K., Nuzzo, R.G., Whitesides, a.G.M., 2005. Chem. Rev. 105 (4), 66.
Lu, B., Smyth, M.R., O'Kennedy, R., 1996. Analyst 121 (3), 29R–32R.
Lum, J., Wang, R., Lassiter, K., Srinivasan, B., Abi-Ghanem, D., Berghman, L., Hargis, B., Tung, S., Lu, H., Li, Y., 2012. Biosens. Bioelectron. 38, 67–73.
Ohno, R., Ohnuki, H., Wanga, H., Yokoyama, T., Endo, H., Tsuya, D., Izumi, M., 2013. Biosens. Bioelectron. 40, 422–426.
Pearson, T.A., Mensah, G.A., Hong, Y.L., Smith, S.C., 2004. Overv. Circ. 110 (25), E543–E544.
Poirier, G.E., Pylant, E.D., 1996. Science 272 (5265), 1145–1148.
Porter, M.D., Bright, T.B., Allara, D.L., Chidsey, C.E.D., 1987. J. Am. Chem. Soc. 109 (12), 3559–3568.
Reddy, P.J., Sadhu, S., Ray, S., Srivastava, S., 2012. Clin. Lab. Med. 32 (1), 47–72.
Roberts, W.L., Moulton, L., Law, T.C., Farrow, G., Cooper-Anderson, M., Savory, J., Rifai, N., 2001. Clin. Chem. 47 (3), 418–425.
Roberts, W.L., Sedrick, R., Moulton, L., Spencer, A., Rifai, N., 2000. Clin. Chem. 46 (4), 461–468.
Romaner, L., Heimel, G., Ambrosch-Draxl, C., Zojer, E., 2008. Adv. Funct. Mater. 18 (24), 3999–4006.
Sassolas, A., Blum, L.J., Leca-Bouvier, B.D., 2012. Biotechnol. Adv. 30 (3), 489–511.
Sondag-Huethorst, J.A.M., Fokkink, L.G.J., 1995. Langmuir 11 (6), 2237–2241.
Trasatti, S., Petrii, O.A., 1991. Pure Appl. Chem. 63, 711–734.
Trilling, A.K., Beekwilder, J., Zuilhof, H., 2013. Analyst 138 (6), 1619–1627.
Ulman, A., 1996. Chem. Rev. 96 (4), 1533–1554.
Wink, T., Zuilen, S.J.V., Bult, A., Bennekom, W.P.V., 1997. Analyst 122 (4), 43R–50R.